Applied Physics B (2023) 129:9
https://doi.org/10.1007/s00340-022-07951-3

**Applied Physics B**
**Lasers and Optics**

RESEARCH

# Intra-cavity immersion diffuser for low-coherence generation in dye and solid-state lasers

**Olga Burdukova[1,2] · Evgeniy Cheshev[1] · Alexey Koromyslov[1] · Vladimir Petukhov[1] · Yuri Senatsky[1] · Ivan Tupitsyn[1]**

Received: 22 October 2022 / Accepted: 29 November 2022 / Published online: 9 December 2022


**Abstract**
A cuvette with a dense immersion mixture of LiF microparticles and isobutyl alcohol was used in resonators of dye and Nd:YAG lasers as a small-angle diffuser to obtain low-coherent generation. Beams with the degree of spatial coherence $\gamma \leqslant 0.1$ were obtained at the output of PM567; Rh101; DCM dye lasers with a cuvette-diffuser under pumping by 532 nm/25 ns single shot pulses, and in Nd:YAG laser with a diffuser under 808 nm QCW LD pumping when controlling the state of immersion in the cuvette. Illustrations of laser beam profiles at changes in the temperature, radiation wavelength or the mixture composition in the cuvette are presented. Temperatures corresponding to the diffuser "initial state" with the maximum level of immersion and cuvette transmission for different laser wavelengths in the visible and near-IR spectral regions were defined. A phenomenological model describing the operation of a laser with a diffuser in the "working state" (low-coherent lasing) is considered. The possibility of use of an immersion diffuser to obtain low-coherence output in dye and solid-state lasers at various wavelengths in the visible and near-IR spectral regions is discussed.

## 1 Introduction

Low-coherence lasers have attracted the attention of researchers since the first publications on this topic in the 1960 s and up to the present time, as such lasers find numerous applications in scientific and applied research and development [1–10]. Various laser devices were tested to form beams with limited coherence. Short pulse powerful Nd:glass lasers with a controllable function of mutual coherence were proposed for the study of the interaction of radiation with matter and ICF experiments [3, 4]. Low-coherence laser sources with relatively moderate power and energy for laser imaging, high speed photography, photolithography based on fiber lasers, Nd:YAG lasers with a degenerate resonator, lasers with a chaotic mode structure, random lasers have been reviewed in [7]. In the works [11, 12] we presented a method to obtain low coherent output beams in dye lasers of 550–650 nm spectral region using in their resonators a cuvette containing a mixture of solid-state micro-particles (LiF crystal pieces) and an immersion liquid with dissolved dye. Such a cuvette is similar in its characteristics to the well-known Christiansen filter, in which the slurry-like dense mixture deflects (scatters) randomly the radiation at small angles due to refraction of the transmitted radiation at the boundaries of particles and liquid. Thus, an intra-cavity cuvette performed in the laser resonator the function of not only the active element, but also a diffuser. It is assumed that such an immersion diffuser split the laser beam in a resonator into fragments—mutually incoherent generation channels. Hence, conditions were created for the formation in the common laser beam a spatially incoherent radiation field.

This article is devoted to an immersion diffuser on a mixture of solid micro-particles and a liquid and its applications in dye and solid-state laser resonators for obtaining low-coherence lasing. Experimental and calculated data and illustrations (including some data from [11–13]), which characterize the parameters of a diffuser on a mixture of LiF particles and isobutyl alcohol (LiF/iso) are presented: the transmission spectrum of a cuvette with a mixture, dependences of the refractive indices of the mixture components on the wavelength, loss coefficients, etc. Temperatures corresponding to the LiF/iso diffuser "initial states" with the maximum levels of immersion and the mixture transmission for

✉ Olga Burdukova
burdukovaoa@lebedev.ru

[1] Division of Quantum Radiophysics, P.N. Lebedev Physical Institute of the Russian Academy of Sciences (LPI RAS), Moscow 119991, Russia

[2] I.M. Sechenov First Moscow State Medical University, Moscow 119991, Russia

different laser wavelengths in the visible and near-IR spectral regions were defined. A model describing the operation of a laser with a diffuser in the "working state" (low-coherent lasing) is considered. Parameters of PM567; Rh101; DCM dye lasers with a diffuser under pumping by 532 nm/ 25 ns pulses and of Nd:YAG laser with a diffuser under 808 nm LD QCW pumping, including coherence measurements, are presented. Illustrations of the rearrangement of output laser beam profiles at changes in the temperature, radiation wavelength or mixture composition in the diffuser are provided. The possibility of using an immersion diffuser on a mixture of micro-particles and liquid to obtain low-coherence output in lasers in the wide regions of visible and near-IR spectra is discussed.

## 2 Immersion diffuser on a mixture of LiF microparticles and isobutanol

Table 1 presents the refractive indices of several known solid-state laser media and optical materials as well as of a number of liquids that can be used in immersion mixtures.The preparation of immersion mixtures with particles of such laser materials as Nd:YAG crystal ($n_D = 1.82$), Nd:$YVO_4$ crystal ($n_o = 1.9573$, $n_e = 2.1652$) and a number of others meets certain difficulties associated with the selection and practical use of liquids with high values of $n$, which are often rather aggressive substances. In our work, we limited ourselves to materials with $1.3 < n < 1.65$, which are included in the Table 1. The choice of LiF granules for the experiments was due to a good combination of this crystal's characteristics. LiF has a high thermal conductivity (4 $Wm^{-1}K^{-1}$), cubic symmetry and its low refractive index, $n_D = 1.39$ at $\lambda_D = 589$ nm, simplifies the selection of the immersion components from a wide range of liquids.

For the preparation of a slurry-like medium, LiF crystal powders were produced by crushing a bulk crystal with subsequent sieving of the material through calibrated sieves. Granules with sizes of 70–140$\mu$m were chosen for the diffuser. Fractions of crushed material were placed and poured with the liquid into rectangular quartz cuvettes (1 or 2 mm gap), so that a layer of the liquid without granules with a height of 1–2 cm was formed above the slurry, Fig. 1a.

As the Table 1 data show, one of the good immersion liquids for LiF is isobutyl alcohol, the refractive index of which ($n_D = 1.39$) is very close to that of LiF. The dispersion curves of the LiF crystal and isobutanol were calculated according to the data [14, 15] and shown in Fig. 1b. The curve of isobutanol at $T = 300$ K was constructed according to [14], and the curve for LiF at $T = 297$ K according to [15]. Since the refractive index of LiF varies little with temperature, the data on LiF at $T = 297$ K may be used in calculations at other temperatures. The coefficient $(dn/dT)$ of isobutanol (iso) is much higher than that of LiF. Therefore, when calculating the indices $n_{iso}$ for different temperatures, corrections should be made to the $n_{iso}$ value at 300 K, using $(dn/dT)_{iso} = 5 \times 10^{-4} K^{-1}$ [12, 14]. As can be seen from Fig. 1b, in the temperature range close to room temperatures, the difference in the refractive indices $\Delta n$ of LiF and isobutanol in a wide range of wavelengths in the visible and near IR regions of the spectrum may be $\leqslant 10^{-3}$.That makes it possible to use LiF and isobutanol for the preparation of mixtures with the high immersion level. It also follows from the data in Fig. 1b that the state of immersion in the LiF/iso mixture will change with the temperature of the mixture and the radiation wavelength. The state of immersion in the

**Table 1** Refractive indices of several solid-state laser media and optical materials

| Material | Refractive index, $n$ | | |
|---|---|---|---|
| | $\lambda = 650$nm | $\lambda = 589$nm | $\lambda = 1060$nm |
| Acetone | 1.3574 | | 1.3526 |
| Ethanol | 1.3600 | | 1.3548 |
| Heptane | 1.3872 | | 1.3827 |
| LiF | 1.3910 | | 1.3866 |
| Isobutyl alcohol | 1.3913 | | 1.3862 |
| Carbon tetrachloride | 1.4545 | 1.4569 | 1.4482 |
| Fused silica | 1.4565 | 1.4584 | 1.4497 |
| Nd:YLiF | 1.4524(o), 1.4750(e) | | 1.4480(o), 1.4702(e) |
| Glycerol | 1.4701 | | 1.4631 |
| Toluene | 1.4926 | | 1.4813 |
| Benzyl alcohol | 1.536 | | |
| Anise oil | 1.560 | | |
| Nd:glass | | | 1.55 |
| $NdP_5O_{14}$ | | 1.60 | |
| Cinnamaldehyde | | 1.62 | |

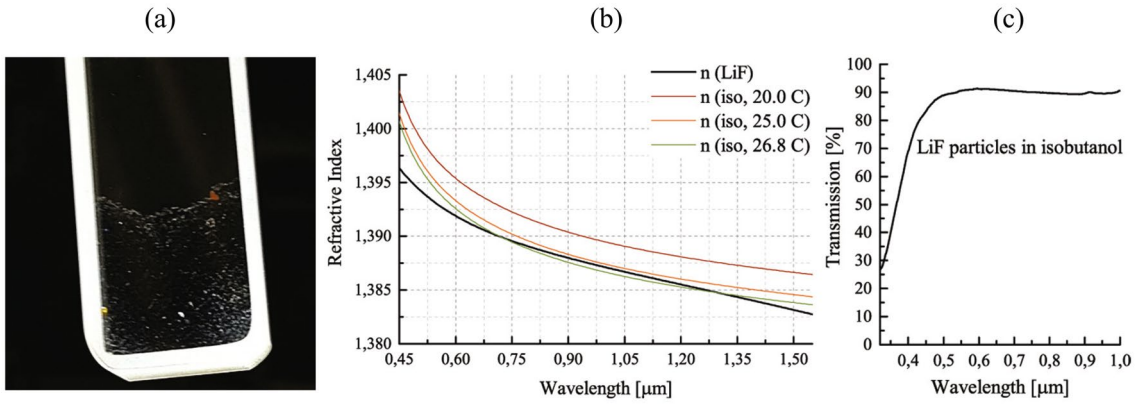


**Fig. 1** **a** Photo of the cuvette with slurry of 70–140$\mu$m LiF granules in an immersion liquid. **b** Dispersion curves of LiF crystal and isobutyl alcohol refraction indices at room temperatures. **c** Transmission spectrum of the 2 mm cuvette with LiF/iso mixture (relative to pure isobutanol)

cuvette can be changed also by additions of auxiliary liquid to the mixture.

Fig. 1c shows the transmission spectrum of the 2 mm cuvette with LiF particles in isobutanol. Isobutyl alcohol is transparent in the visible spectrum, and its absorption in the near IR at about 1 $\mu$m, where the neodymium laser generation lines are located, is small. In the spectral region from 600 nm to 1000 nm, the mixture transmits 80–90% of the radiation incident on the cuvette. Transmission decay at short wavelengths is a result of light scattering.

Figs. 2, 3 illustrate the operation of a cuvette-diffuser (2 mm gap) outside the resonator using an auxiliary He-Ne laser beam ($\lambda \approx 633$ nm). To get away from the high immersion state and increase the scattering, small amounts of ethanol ($n_D = 1.36$) or acetone ($n_D = 1.36$) can be added to the mixture. The spots of the He-Ne laser beam, which passed through the cuvette-diffuser at 3 different compositions of the medium at the temperature $T \approx 300$ K, are shown in Fig. 2. In Fig. 2a, the laser beam passes a pure isobutanol layer practically without distortions. At the same time a beam passage through the slurry is accompanied by an increase in graininess of the laser spot and in the beam divergence as immersion deteriorates, Fig. 2b, c.

To characterize the cuvette-diffuser, we use the difference in the refractive indices of particles and liquid, $\Delta n$, the attenuation coefficient $\alpha$, which describes the scattering (refraction) losses in the slurry and the deflection angle $\psi$ of the laser radiation after the cuvette. The diffuser parameters were estimated in the experimental set-up with He-Ne laser shown in Fig. 3a. A parallel ∅4 mm He-Ne laser beam was directed to a cuvette (2 mm gap) with the slurry of LiF particles. The beam that passed through the cuvette was directed to a lens, in the focus of which a diaphragm was installed, and behind it a detector. A lens with a focal length $f = 2.1$ m and ∅1.3 mm diaphragm were used, that corresponds to a detection angle of 0.6 mrad.

The intensity of the radiation transmitted by the slurry was compared with the intensity of the beam transmitted

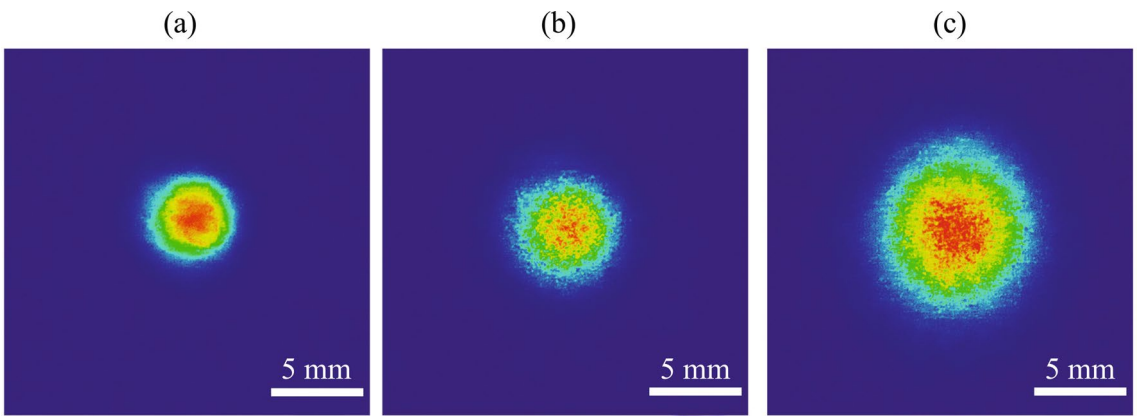


**Fig. 2** He-Ne laser beam spots at the screen 17 cm behind the cuvette (2 mm gap) at $T \approx 300$ K. Initial laser beam diameter is ≈2 mm. Cuvette filling: **a** pure isobutanol; **b** LiF/iso; **c** LiF/iso + acetone (10:1)

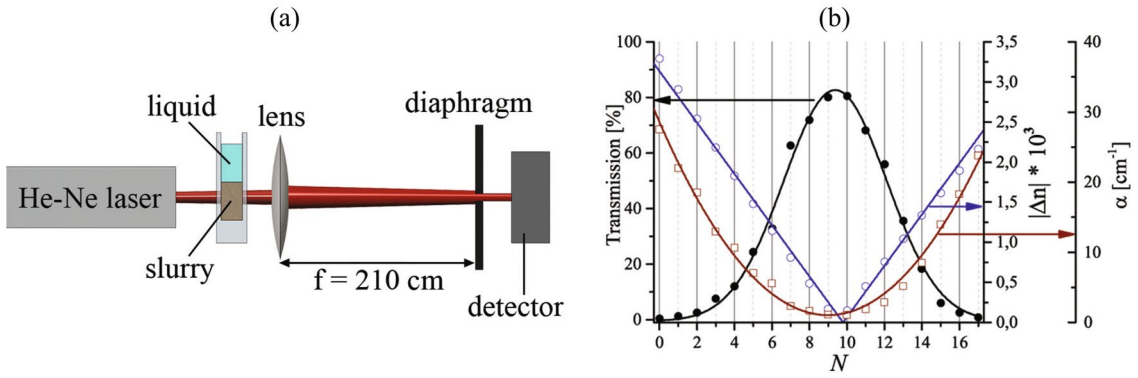


**Fig. 3** **a** Scheme of the experiment on registration of transmission and losses of radiation at $\lambda = 633$ nm during the passage of a He-Ne laser beam through a cuvette-diffuser. **b** Dependences of transmission, loss coefficient and the difference in the refractive indices of particles and liquid, $\Delta n$ at $\lambda = 633$ nm in 2 mm thick LiF/iso slurry (70–140 $\mu$m particles) on ethanol drops additions, $N$ (T ≈ 293 K)

through the liquid layer above the particles, which was taken as 100%. Unlike Fig. 2, this experiment was carried out at a temperature of ≈293 K, at which the initial transmission of the cuvette with LiF particles in isobutanol for a given detection solid angle was close to zero. To change the immersion, ethanol was added dropwise ($V_{drop} \approx 0.006$ ml) to the isobutanol ($V_{iso} \approx 0.55$ ml), and the transmission was measured for each next drop. The maximum transmission (≈ 80%) was achieved when 9–10 drops of ethanol were added. Then, with each new drop, the transmission decreased and became almost 0 at the 18th drop. The dependences of the transmittance and corresponding calculated loss coefficients $\alpha$ on number of drops $N$ are shown in Fig. 3b. The refractive indices difference $\Delta n$ was calculated according to the data [14, 15]. As can be seen from the graphs in Fig. 3b, the $\Delta n$ values vary depending on the immersion level in the range $(0.1–3.5)\times10^{-3}$, and the loss coefficient $\alpha$ takes the values $1 - 25\ \mathrm{cm}^{-1}$. So it can be seen that rather small changes in $\Delta n$ may lead to significant scattering losses. Measurements of the deflection angles $\psi$ of the He-Ne laser radiation after the cuvette were carried out with a short-focus lens according to a scheme similar to Fig. 3a [12]. For a high level of immersion, the $\psi$ values did not exceed 3 mrad and reached 40 mrad for a poor immersion.

The experiments performed with the He-Ne laser gave grounds to assume that when a cuvette-diffuser with the LiF/iso mixture is installed in the laser of a certain wavelength, it will be possible to adjust the level of scattering in the diffuser by small additions of an auxiliary liquid or by changing the temperature and to go from the "initial state" with the maximum level of immersion and coherent lasing to the low immersion "working state" and the low-coherence generation. For different radiation wavelengths, the LiF/iso mixture without additives will provide a high immersion state of the diffuser, obviously at different temperatures. For our experiments dye lasers operating in the visible region of the spectrum PM567 (567 nm); Rh101 (598 nm) or DCM (626 nm) and the Nd:YAG laser (1064 nm) were used. To determine the temperatures corresponding to the initial states of the diffuser for these selected dye laser media and for the Nd:YAG laser, calculations were made using refractive index dispersion data [14, 15]. The dispersion curves of the LiF and isobutanol were plotted for a small region of the visible spectrum 550–650 nm, Fig. 4a. Figure 4b shows the dispersion curves of LiF and isobutanol for the 700–1300 nm region, where the Nd:YAG as well as Yb:YAG and polymethine IR dye lasers lines are located. The initial states of immersion in the mixture correspond to the intersection points of the LiF and isobutanol dispersion curves.

Figure 5 shows the dependence of the found temperatures of the LiF/iso immersion mixture "initial states" on the wavelength. It can be seen that with the transition from the IR region to the short wavelengths, the temperatures of the "initial states" change from 25 to 39°C.

The data presented at Figs. 4, 5 may be used as guidelines in choosing the experimental conditions for obtaining generation in lasers with a LiF/iso diffuser. Exact observance of temperatures indicated in Figs. 4, 5 and obtaining coherent generation in dye and solid-state lasers exactly at the points of initial states of the LiF/iso diffuser were not our task. Experiments with dye and Nd:YAG lasers started as a rule at small detuning in the temperature or mixture compositions from an initial state. Then, usually, by adding an auxiliary liquid to the mixture, the diffuser was transferred to the working state, which ensured low-coherence generation in the laser. The following section presents pictures illustrating the operation of the dye and Nd:YAG lasers with an LiF/iso diffuser and the transitions between different operating states of these lasers under changes in the mixture composition, as well as under changes in the temperature and the radiation wavelength. Estimations of the change in the

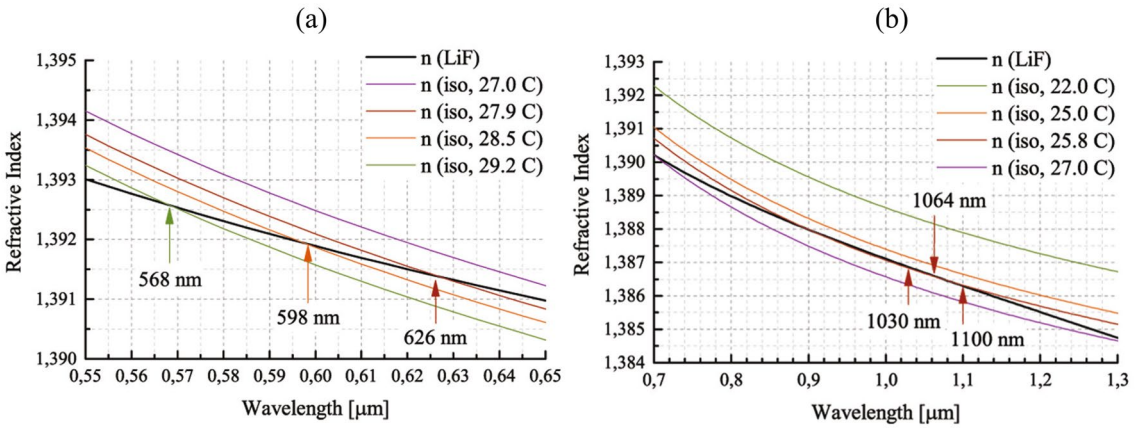


**Fig. 4** Dispersion curves of LiF and isobutanol refractive indices: **a** 550–650 nm; **b** 700–1300 nm region

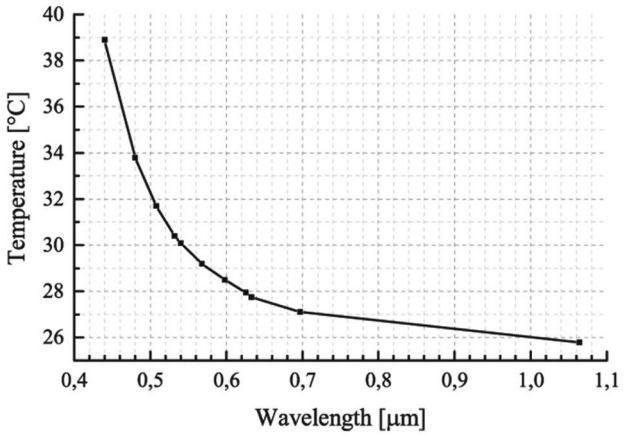


**Fig. 5** Dependence of the temperatures of the LiF/iso immersion mixture "initial states" on wavelength

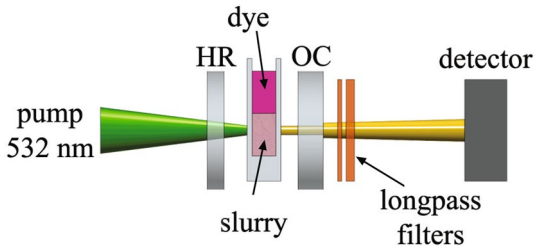


**Fig. 6** Schematic of the experiment on the excitation of lasing in a slurry of LiF particles (70–140 $\mu$m) with a solution of a dye in isobutanol

refractive indices difference in the diffuser, $\Delta n$, during the transition from coherent lasing to the low-coherence generation according to the data of the work [12] is $\Delta n \approx 2 \times 10^{-3}$.

## 3 Generation in dye and Nd:YAG lasers with an intra-cavity diffuser

Lasing in a 2 mm cuvette containing LiF particles in isobutanol with a dye was excited by 25 ns pulses of the 2nd harmonic of a multimode Nd:YAG laser (532 nm). The cuvette was installed in a 2 flat mirrors resonator, Fig. 6. Experiments were carried out at temperatures $T$ = 295–300 K with PM567; Rh101 or DCM dyes, which lase in spectral regions centered, respectively at 568 nm; 598 nm; 626 nm. A pump pulse of up to 17 mJ was slightly focused into a slurry volume with a dye in the cuvette. The focusing spot diameter was ≈2 mm, and the pump intensity reached $2 \times 10^7$ W/cm$^2$. A laser with an active medium in the form of a slurry can be called a "slurry laser". Operation of a slurry laser with solutions of PM567; Rh101 or DCM dyes in isobutanol was obtained in the resonator with the base, $L$ = 2.5 cm. We used mirrors with reflection coefficients: HR mirror: $R$(532 nm) = 8.1%, $R$(568 nm) = 80%, $R$(598 nm) = 99.8%, $R$(626 nm)> 99.9%; OC: $R$(568 nm) = 65.8%, R(598 nm) = 62.7%, R(626 nm) = 57.4%. The pump radiation not absorbed by the dye was cut off from the output laser beam by filters. To compare the characteristics of slurry dye lasers with those of lasers based on the same dyes, but without particles, the cuvette was moved down and the pump beam was focused into the dye solution above the layer of LiF granules. Let us call such lasing as DL (dye laser).

The energy of 10–20 ns pulses of the slurry dye lasers reached 1 mJ and the DL pulses energy reached 4 mJ. The lasing efficiencies of slurry lasers and DLs reached 7% and 16%, respectively. The generation band width of these lasers was 2–3 nm. Output parameters of slurry lasers with PM567, Rh101, and DCM dyes (intensity profile, beam divergence, lasing spectrum, state of coherence) had

significant differences, which are associated with the difference in the refractive indices of particles and liquids $|\Delta n|$ for the spectral regions in which dyes lase as well as with the dependence $|\Delta n|$ on temperature and the slurry composition. The Figs 7– 11 illustrate the work of dye slurry lasers and their transitions between different operation states.

Figure 7 shows photo of the Rh101 dye slurry laser output in the far field (at the focus of a lens, $f \approx 2$ m), which illustrate the transformation of the beam profile under the temperature shift. At a high level of immersion (pure isobutanol, $T \approx 300$ K) clear structures of rings with a bright central core were observed, Fig. 7a. The divergence of the beam central region was 5.2 mrad, and the divergence (full angle) of the first 4 rings was 11.4; 16.0; 19.6; 22.6 mrad. The location of rings along the angular coordinate corresponded to the transmission maxima of a Fabry-Perot interferometer (FPI) formed by resonator mirrors, Fig. 7b. The transmittance maxima of the FPI for a diverging beam at a wavelength $\lambda$ correspond (as is well known) to the directions for which the optical path length in the FPI differs by an integer number of wavelengths, n$\lambda$ ($n = 1;2$ ...) according to the formula [12]

$$I = \frac{I_0 T^2}{(1-R)^2 + 4R\sin^2\left(\frac{2\pi L\cos(\theta/2)}{\lambda} + \phi\right)}. \quad (1)$$

Here, $I_0$ is the intensity of the radiation incident on the FPI, $I$ is the transmitted intensity, $\theta$ is the angle of incidence of the radiation, $R$ is the average reflection coefficient and $T$ is the transmittance of the mirrors, $L$ is the FPI base (resonator length), and $\phi$ is the phase. So, the observed rings were obviously the result of the interference of coherent radiation in the FP resonator. When the temperature in the cuvette was changed from 300 K to 295 K, the refractive index of isobutanol increased, while the LiF index practically did not change, that is, the immersion level in the cuvette had been lowered. In this case, a beam with a smooth bell-shaped profile without rings was observed at the Rh101 dye slurry laser output, Fig. 7c.

Using a 2-slits Young interferometer, measurements of the spatial coherence of Rh101 dye slurry laser radiation were carried out. The width of each slit was 155 $\mu$m, the distance between their centers was 500 $\mu$m. Figure 8 shows the results of processing the interference patterns of Rh101 dye slurry laser and Rh101 DL radiation at $T = 295$ K. For each of the interferograms, the visibility function (degree of spatial coherence) was calculated $\gamma = (I_{max} - I_{min})/(I_{max} + I_{min})$, where $I_{max}$ and $I_{min}$ are the intensities at the maxima and minima of the interference pattern. As can be seen from Fig. 8, the level of spatial coherence for the multimode Rh101 DL is $\gamma = 0.30$, for Rh101 dye slurry laser $\gamma$ drops to 0.02. The

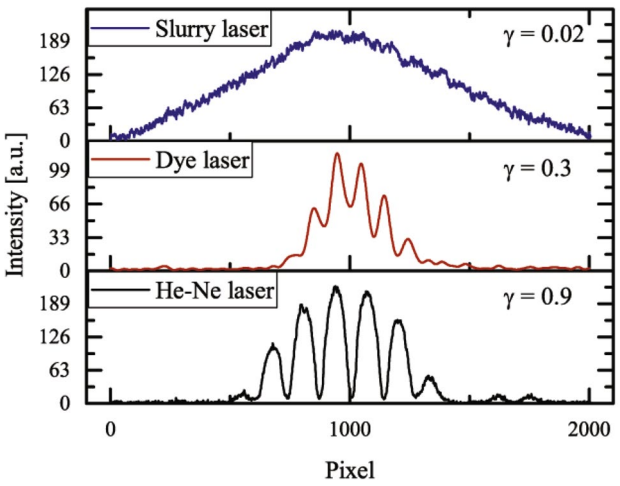


**Fig. 8** Young interferograms of Rh101 slurry laser, Rh101 DL and He-Ne laser

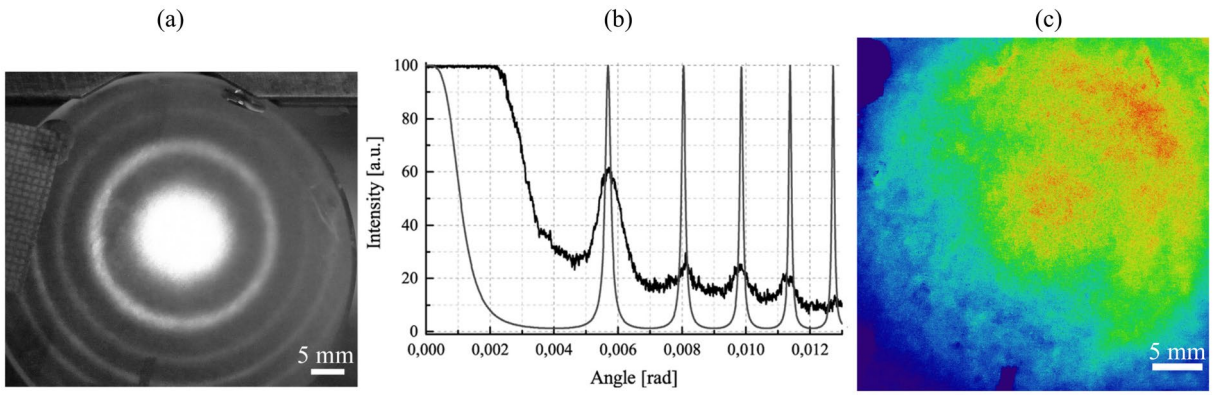


**Fig. 7** Beam profiles of the Rh101 dye slurry laser at the focus of a lens, $f \approx 2$ m: **a** the central core and the ring structure, $T \approx 300$ K. **b** slurry laser output profile with intensity maxima, $T \approx 300$ K (black) and the transmission maxima of the FPI formed by the mirrors (gray). **c** slurry laser output beam profile, $T = 295$ K

bottom fragment of Fig. 8 shows an interferogram from an "ideal" coherent source (single-mode He-Ne laser), where the modulation depth reaches almost 100%, and $\gamma = 0.90$. Thus, looking at the output beam profile of a laser with a FP resonator, one can qualitatively judge the state of laser radiation coherence. The profile with rings makes it possible to speak about the presence of the coherent radiation. The smoothed profile without rings corresponds to low-coherent laser output.

Figure 9 shows photographs of the beams generated by the Rh101 dye slurry laser in the far field (using a lens, $f \approx 2$ m) at a fixed temperature $T = 295$ K, which illustrate the transformation of the beam profile with a change in the composition of the mixture. The photo in Fig. 9a (same as Fig. 7c) corresponds to the dye/LiF/pure isobutanol mixture and low coherent lasing. When then, step by step, the level of immersion was gradually increased by adding drops of ethanol to the cuvette, broadened rings began to appear (Fig. 9b, c) and their width consistently decreased to the state of Fig. 9d, similar the state observed at ≈300 K with pure isobutanol (Fig. 7a).

Figure 10 shows the profiles of dye slurry laser beams in the near field with a change in the radiation wavelength at the fixed temperature and composition of the mixture. This experiment used PM567 and DCM dye slurry lasers operating at $T \approx 300$ K with LiF/pure isobutanol mixture. This composition for PM567 dye slurry laser, operating near 567 nm, provided a smooth beam profile, Fig. 10a.The divergence of PM567 slurry laser radiation reached 80 mrad and

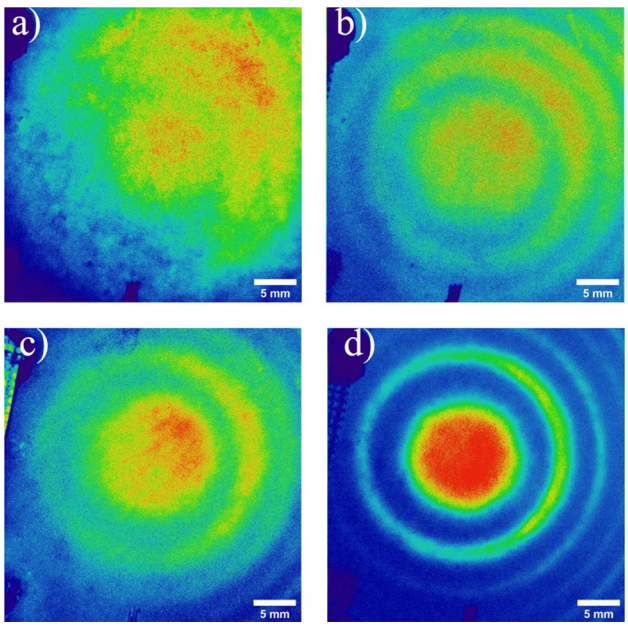


**Fig. 9** Profiles of the Rh101 dye slurry laser beam when changing the composition of the immersion liquid at $T = 295$ K: **a** pure isobutanol; **b**, **c** ,**d** isobutanol + ethanol drops

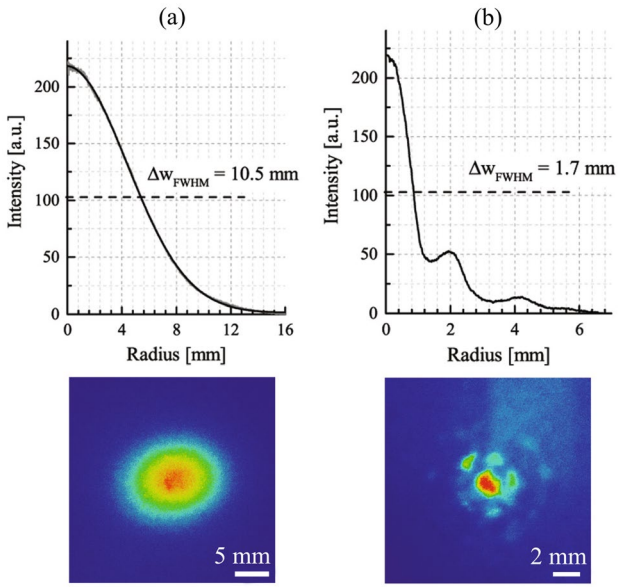


**Fig. 10** Profiles of slurry laser beams in the near field: **a** PM567 dye slurry laser spot at 9 cm distance from the laser; **b** DCM dye slurry laser spot at 33 cm distance from the laser. $T \approx 300$ K

the parameter $\gamma \leq 0.1$. In contrast to the PM567 slurry laser, the DCM slurry laser exhibited ring-structured profiles indicating that the diffuser had entered a state close to the "initial state" for the DCM laser wavelength, Fig. 10b. The angular divergence of the central core of the DCM slurry laser beam was 6.5 mrad, the divergence of the first ring was 11.7 mrad.

In the work with the Nd:YAG laser, the 2 flat mirrors resonator with an internal lens was used to suppress ring structures in the laser output, Fig. 11. The experiments were carried out with a Nd:YAG rod ∅4 × 5 mm (1% activator concentration), one end of which was polished to a sphere of radius $R = 100$ mm and antireflection coated. A dichroic mirror M1 with ≈ 100% reflection for $\lambda = 1064$ nm and 96% transmission for pumping wavelength, $\lambda = 808$ nm was deposited on the other flat end. This mirror, together with a flat mirror M2 with a transmission of 4% at $\lambda = 1064$ nm, formed a resonator with a length $L = 21$ mm .

Pumping was carried out by a 100 W Dilas diode module in QCW regime with the pump pulse frequency ≈ 10 Hz. About 80% of the pump energy was absorbed in the Nd:YAG rod and a gain channel with a diameter of up to 1 mm was formed in the rod along the resonator axis. The experiments were carried out with the thermal control at a temperature 25°C, which is close (according to Figs. 4b, 5) to the diffuser high immersion state for $\lambda = 1064$ nm. The power in ≈1 ms laser pulses was 10–200 mW, depending on the level of immersion in the diffuser. Registration of laser beam profiles was carried out using Thorlabs BC106-VIS CCD camera (registration window 6.6 × 8.8 mm). In the case of high immersion, the

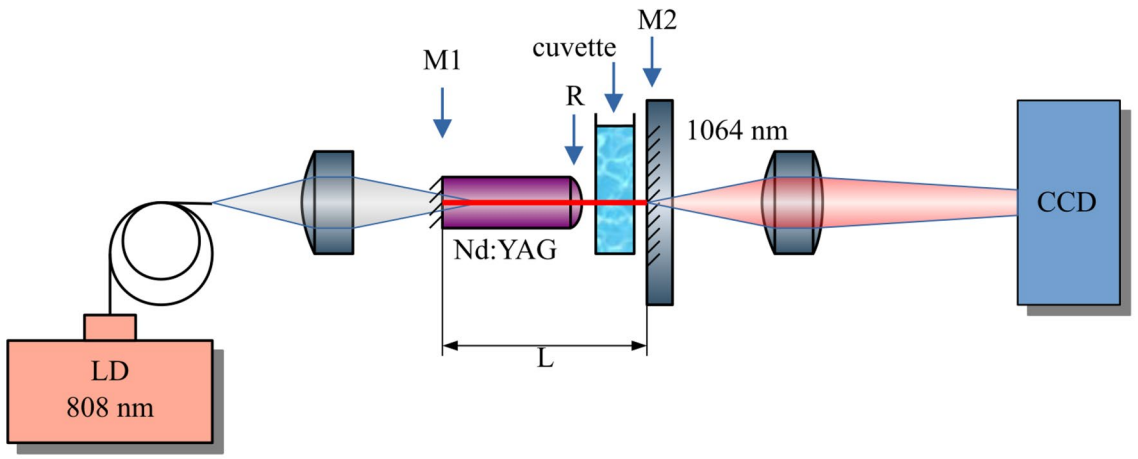


**Fig. 11** Scheme of Nd:YAG laser with a diffuser. *M1, M2* mirrors, *LD* pump module, *CCD* camera

beam profile at the output of the laser practically repeated the profile of single-mode lasing, Fig. 12a. The presence of a lens in the active element made it possible to exclude the ring structures on the laser beam profile. The profiles of the laser beams in the near and far fields in the case of poor immersion in the diffuser are shown in Fig. 12b, c.

The studies of the spatial coherence of the Nd:YAG laser with a diffuser were carried out using the same Young interferometer. The obtained values of the $\gamma$ parameter for a Nd:YAG laser with a diffuser (LiF/iso + 8 ethanol drops) and without it are $\gamma = 0.10$ and $\gamma = 0.76$. Note that the obtained low coherence Nd:YAG lasing in QCW regime suggests that low-coherence generation in a Nd:YAG laser can also be obtained under laser pumping with ns pulses, similar to pulsed pumping of slurry dye lasers.

## 4 Discussion

The presented illustrations show the possibility of using an immersion diffuser to obtain low-coherence generation with a visibility parameter $\gamma \leq 0.1$ in dye and solid-state lasers. The data obtained make it possible to offer a mechanism of generation in a laser with an immersion diffuser at various levels of immersion that explains the rearrangement of the output laser radiation patterns. At a high level of immersion in the diffuser near its "initial state", the variations in the optical thickness, $\Delta S$ when light passes through a diffuser in different places are small and a slightly distorted fundamental mode can arise, forming the generation core. In a laser with a FP resonator, coherent radiation interferes during scattering. It is suppressed along the directions near the FP transmission minima and gets stronger along the directions of FP transmission maxima. The output radiation pattern with rings is formed in this case, Fig. 7a, b. At very low

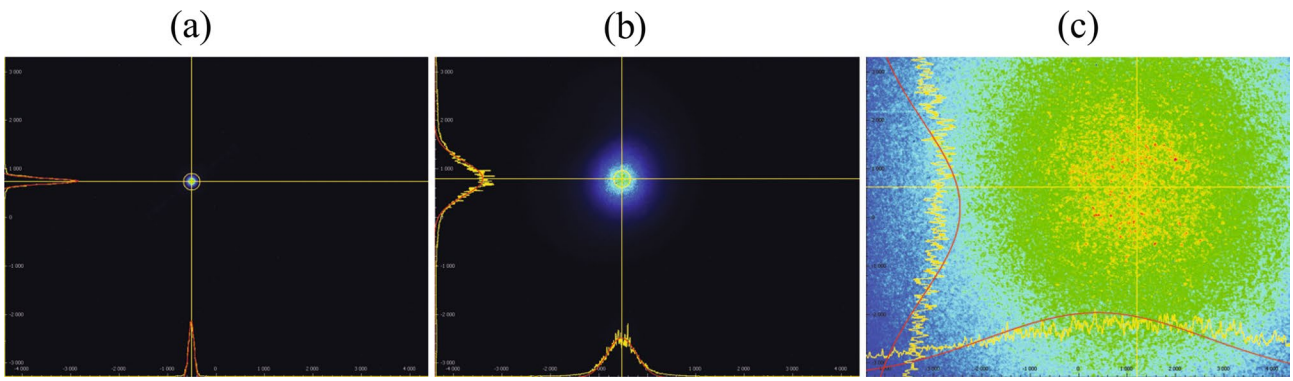


**Fig. 12** **a** Beam profile of the Nd:YAG laser at the output mirror; **b**, **c** beam profiles of the Nd:YAG laser with 2 mm cuvette-diffuser (LiF/iso + 8 drops of ethanol) at the output mirror (**b**) and in the focus of a lens, $f = 60$ mm (**c**)

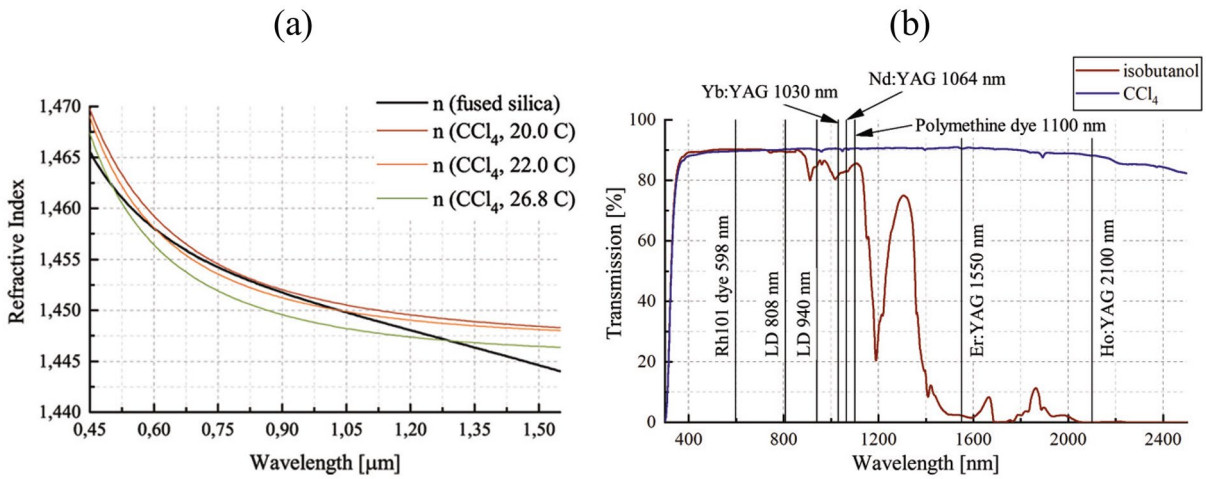


**Fig. 13** **a** Dispersion curves of fused silica and $CCl_4$ refractive indices . **b** Transmission of isobutanol or $CCl_4$ in a 1cm thick glass cuvette in the visible and near IR spectral regions. Locations of the generation and pump lines of a number of laser media are shown

immersion, the variations in the optical thickness, $\Delta S$ are significant. Due to the refraction of radiation at numerous interfaces between particles and liquid and chaotic deflection of small beam parts, independent generation channels with small cross-sections differing in an optical length are appeared in the resonator. The mutual spatial coherence of such channels is obviously broken. All these channels form a common spatially incoherent beam core with a smooth profile. Since radiation of very low coherence from this core circulates in the resonator, it does not interfere during scattering and spreads at the laser output in the directions of maxima or minima of the FP resonator transmission and in the intermediate directions without attenuation. In this way, a smoothed common laser beam profile with a large angular divergence is formed, Fig. 7c. Similar processes should also occur in a resonator with a lens (or in a plano-spherical resonator), leading to the formation of a smoothed, spatially incoherent laser beam profile, Fig. 12b, c. There are no rings in this case.

The transition of a laser with a diffuser near the "initial state" to low-coherence generation can be carried out, as shown in Section 3, by changing the temperature, the radiation wavelength, and the composition of the mixture. An illustration of such a transition with a change in the composition of the mixture is shown for Rh101 dye slurry laser with a FP resonator, in Fig. 9. With an intermediate immersion level, it can be assumed that among the many generation channels there are a number of rather large lasing regions with moderate variations in the optical thickness, $\Delta S$, which allow the development of coherent generation. For a laser with an FP resonator, emission from different such regions form ring structures at the output of the laser at different angles due to the spread of optical thicknesses $S$, which leads to broadening of the interference rings, Fig. 9b, c. The gaps between rings are filled with incoherent background radiation from the rest generation channels in the mixture. One can say that in this case we are dealing with partially coherent radiation at the laser output.

Note that the proposed scheme of a low-coherence laser with an immersion diffuser can be used not only with the tested dye and Nd:YAG lasers, but also with other solid-state and dye lasers in the visible and near-IR range operating in pulsed and QCW modes. Discussing the prospects for lasers with an immersion diffuser, one should point out the need for further work on optimizing pumping schemes, increasing the laser efficiency, and also on methods for controlling the coherence level in laser beams. Speaking about the optimization of the immersion composition itself, one more immersion pair for creating a diffuser should be pointed out: a mixture of particles from fused quartz and liquid carbon tetrachloride, $n \approx 1.45$ (Table 1). Fig. 13a shows the dispersion curves of this mixture, indicating the possibility of obtaining a high level of immersion in the diffuser in both the visible and near-IR ranges. When constructing these curves, data on the dispersion of fused quartz and carbon tetrachloride (taking into account their temperature dependences) from the works [14, 16] were used. In contrast to isobutanol, $CCl_4$ has negligible absorption in the near-IR range usually caused by vibration bands of hydrogen atoms in organic molecules, Fig. 13b. Fused quartz is transparent in the IR region up to almost 3500 nm. This will reduce the cavity loss and can help limit the heat release in the immersion mixture and increase the average radiation power in lasers with a diffuser. The good transparency of $CCl_4$ and fused silica in the IR region makes it possible to consider the possibility of excitation of low-coherence generation (using an immersion diffuser) in such well-known solid-state laser media as Er:YAG, operating near 1550 nm, Tm:YAG, Tm:YLF and Ho:YAG,

Ho:YLF, operating at wavelengths around 2000 nm, where isobutanol is unsuitable. Figure 13b shows the locations of the generation and pump lines of a number of laser media relative to the transmission spectra of isobutanol and $CCl_4$.

## 5 Conclusion

This paper presents the usage of an intra-cavity immersion diffuser based on a cuvette with dense mixture of LiF microparticles and isobutyl alcohol in dye and Nd:YAG lasers to obtain low-coherence laser output (visibility parameter $\gamma \leq 0.1$). Temperatures corresponding to the diffuser "initial state" with the maximum level of immersion and cuvette transmission for different laser wavelengths in the visible and near-IR spectral regions were defined. Generation in PM567; Rh101; DCM dye lasers with a diffuser was obtained under pumping by 532 nm/25 ns pulses, and in Nd:YAG laser with a diffuser under 808 nm LD QCW pumping. Illustrations of the laser beam profiles at changes in the temperature, radiation wavelength or the mixture composition in the diffuser are presented. A phenomenological model describing the operation of a laser with a diffuser in the "working state" (low-coherent lasing) is considered. The possibility of use of an immersion diffuser to obtain low-coherence output in lasers in the wide regions of visible and near-IR spectra is shown.

**Acknowledgements** The authors thank P.G. Zverev and V.A. Konyushkin for help in preparing the components of immersion solutions and studying their characteristics.

**Author contributions** BOA: calculations and construction of dependences of the refractive indices of the LiF/iso diffuser components and its operating temperatures on the wavelength, processing the results of laser experiments, preparing the text of the manuscript and figures for publication. BOA, PVA, SYV: study of characteristics of immersion LiF/iso diffuser, experiments on dye lasers with LiF/iso diffuser. KAL, SYV, TIM, CEA : experiments with NdYAG laser with immersion LiF/iso diffuser, processing of experimental results, preparation of figures 11,12,13. BOA., KAL, SYV, PVA: wrote the main manuscript text. All authors reviewed the manuscript.

## Declarations

**Conflict of interest** The authors declare that they have no competing interests.

## References

1. R. Ambartsumyan, N. Basov, P. Kryukov, V. Letokhov, A laser with a nonresonant feedback. IEEE J. Quantum Electron. **2**(9), 442–446, (1966). https://doi.org/10.1109/JQE.1966.1074123
2. V.S. Letokhov, Generation of Light by a Scattering Medium with Negative Resonance Absorption. Sov. J. Exp. Theor. Phys. **26**, 835, (1968)
3. M. Nakatsuka, N. Miyanaga, T. Kanabe, H. Nakano, K. Tsubakimoto, S. Nakai, Partially coherent light sources for ICF experiment. In: Photonics West - Lasers Appl. Sci. Eng. (1993)
4. S. Fedotov, L. Feoktistov, M. Osipov, A. Starodub, Lasers for ICF with a controllable function of mutual coherence of radiation. J. Russ. Laser Res. **25**(1), 79–92, (2004)
5. B. Redding, M.A. Choma, H. Cao, Speckle-free laser imaging using random laser illumination. Nat. Photonics. **6**(6), 355–359, (2012)
6. M. Nixon, B. Redding, A. Friesem, H. Cao, N. Davidson, Efficient method for controlling the spatial coherence of a laser. Opt. Lett. **38**(19), 3858–3861 (2013)
7. H. Cao, R. Chriki, S. Bittner, A.A. Friesem, N. Davidson, Complex lasers with controllable coherence. Nat. Rev. Phys. **1**(2), 156–168 (2019). https://doi.org/10.1038/s42254-018-0010-6
8. Y. Wang, X. Ji, Z. Chen, J. Pu, Q-switched partially coherent lasers with controllable spatial coherence. Opt. Appl. **51**, 245–256 (2021)
9. K.-S. Lee, H.J. Ma, F. Rotermund, D.K. Kim, Y. Park, Non-resonant power-efficient directional Nd:YAG ceramic laser using a scattering cavity. Nat. Commun. **12**, 8 (2021)
10. A.W. Steinforth, J.A. Rivera, J.G. Eden, Imaging of transient phenomena with low coherence lasers comprising arrays of independent microbeams: A laser version of Harold Edgerton's stroboscope. APL Photonics **7**(1), (2022). https://doi.org/10.1063/5.0076899
11. O. Burdukova, V. Petukhov, Y. Senatsky, Lasing in a medium with the properties of a Christiansen filter. Opt. Lett. **45**(12), 3236–3239, (2020). https://doi.org/10.1364/OL.394276
12. O.A. Burdukova, V.A. Konyshkin, V.A. Petukhov, M.A. Semenov, Y.V. Senatsky, Low-coherence dye laser with an intracavity radiation diffuser. Opt. Express **29**(8), 11453–11467, (2021). https://doi.org/10.1364/OE.421066
13. O.A. Burdukova, E.A. Cheshev, A.L. Koromyslov, V.A. Petukhov, Y.V. Senatsky, I.M. Tupitsyn, Ring structures in radiation at the output of solid-state and dye lasers with an intra-cavity diffuser. J. Russ. Laser Res. **43**(5), 619–625, (2022)
14. K. Moutzouris, M. Papamichael, S.C. Betsis, I. Stavrakas, G. Hloupis, D. Triantis, Refractive, dispersive and thermo-optic properties of twelve organic solvents in the visible and near-infrared. Appl. Phys. B **116**(3), 617–622, (2014)
15. H.H. Li, Refractive index of alkali halides and its wavelength and temperature derivatives. J. Phys. Chem. Ref. Data. **5**(2), 329–528, (1976). https://doi.org/10.1063/1.555536
16. I.H. Malitson, Interspecimen comparison of the refractive index of fused silica. J. Opt. Soc. Am. **55**(10), 1205–1209, (1965). https://doi.org/10.1364/JOSA.55.001205